J. Appl. Glycosci., **71**, 103−110 (2024)
doi:10.5458/jag.jag.JAG-2024_0007

Regular Paper

Mechanism-based Modelling for Fitting the Double-exponential Progress Curves of Cellulase Reaction

(Received May 9, 2024; Accepted July 2, 2024)
(J-STAGE Advance Published Date: October 29, 2024)

Kiyohiko Igarashi,[1,†] Takahiro Ezaki,[2] and Masahiro Samejima[1]

[1] *Department of Biomaterial Sciences, Graduate School of Agricultural and Life Sciences, The University of Tokyo (1−1−1, Yayoi, Bunkyo-ku, Tokyo 113−8657, Japan)*
[2] *Division of Advanced Logistics Science, Research Center for Advanced Science and Technology, The University of Tokyo (4−6−1 Komaba, Meguro-ku, Tokyo 153−8904, Japan)*

Abstract: Enzymatic hydrolysis of cellulosic biomass is a complex process involving many factors, including multiple enzymes, heterogeneous substrates, and multi-step enzyme reactions. Cellulase researchers have conventionally used a double-exponential equation to fit the experimental time course of product formation, but no theoretical basis for this has been established. Here we present a mechanism-based equation that fits well the progress curves of cellulase reaction, incorporating the concepts of non-productive and productive binding on the cellulose surface and processivity. The derived equation is double exponential. Our findings indicate that the reaction mechanism of cellulase itself can account for the double-exponential nature of the progress curve independently of other factors that may contribute, such as substrate heterogeneity and involvement of other enzymes.

Key words: cellulase, glycoside hydrolase, progress curve, biomass utilization

INTRODUCTION

In progressing towards a carbon-neutral society, enzymatic hydrolysis of cellulose is a bottleneck in the production of soluble saccharides such as glucose and cellobiose from non-edible biomass [1]. Cellulase is an attractive option for converting cellulosic biomass because it can hydrolyze cellulose under mild conditions, and it is becoming more widely utilized as recent developments in biotechnology have reduced its cost [2]. Therefore, it is important to understand its mechanism of action in detail to maximize its utility.

Cellulases that act on insoluble cellulose typically consist of two domains, the cellulose-binding (CBD) and catalytic (CD) domains [3, 4]. As shown in Fig. 1, cellulose hydrolysis is typically initiated by the adsorption of the enzyme on the cellulose surface, mediated by the CBD, though the resulting enzyme-substrate complex is "non-productive" because adsorption on cellulose itself does not produce any products [5, 6]. The following reaction is highly dependent on the characteristics of the CD for saccharide production [7, 8], i.e., the cellulose chain is retained after the initial hydrolysis and a further hydrolytic reaction occurs to produce soluble saccharide (typically cellobiose); this is called the "processive reaction" [9]. However, if the CD leaves the chain soon after the initial hydrolysis reaction, the reaction is called "non-processive". Processivity is the key to the degradability of crystalline cellulose by the enzyme [10, 11]. We previously used high-speed atomic force microscopy (HS-AFM) to visualize the processive movement of microbial cellobiohydrolases (CBHs) [12−14] and we discussed the structure-function relationships of CBHs based on the idea of convergent evolution of cellulolytic bacteria and fungi [15]. These recent studies indicate that a combination of cutting-edge biophysical approaches with quantitative biochemical analysis is required to understand the reaction mechanism of the enzyme.

Many biochemical approaches have been used to examine the time course of product formation (the progress curve) by cellulases, but no consistent understanding has emerged, probably because of the complexity of enzymatic cellulose hydrolysis [11, 16]. In early investigations, it was suggested that the heterogeneity of cellulose, i.e., the presence of a mixture of crystalline and amorphous regions, might be important because of the endo-exo theory, i.e., that endo-glucanases (EGs) degrade amorphous regions of cellulose while crystalline cellulose is hydrolyzed by exo-type enzymes later called CBHs [17−21]. Since amorphous regions are quickly degraded by EGs while the degradation of crystalline part is slow, it seems reasonable to apply a two-term equation, such as a double exponential, to fit the progress curves. However, it was found that degradation was biphasic even when a single, highly purified enzyme was applied to highly crystalline cellulose [6, 11]. Thus, it appeared that the fitting of the observations to a double-exponential equation is not simply due to substrate heterogeneity or involvement of multiple enzymes.

†Corresponding author (Tel. +81−3−5841−5255, E-mail: aquarius@mail.ecc.u-tokyo.ac.jp, ORCID ID 0000-0001-5152-7177).
Abbreviations: CBD, cellulose-binding domain; CBH, cellobiohydrolase; CD, catalytic domain; EG, endo-glucanase; GH, glycoside hydrolase; HS-AFM, high-speed atomic force microscopy.

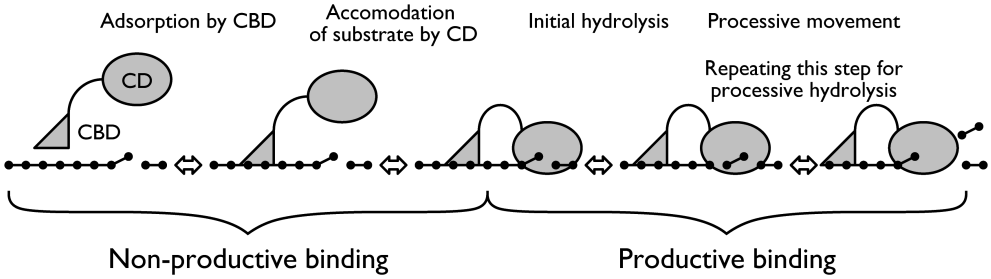

Fig. 1. Mechanism of action of cellulase with a dual domain structure, used to construct the theoretical equation.
CBD, cellulose-binding domain; CD, catalytic domain.

In the present manuscript, we have developed a mechanism-based double-exponential equation that fits well the progress curve of the cellulase reaction, thereby providing a theoretical basis for the observation that the progress curve of cellulase shows a double-exponential character. This approach should be applicable not only to cellulases, but also to other enzymes that act on insoluble substrates with or without processivity.

MATERIALS AND METHODS

The theoretical development is presented step-by-step in the following Results and Discussion section. The kinetic data of glycoside hydrolase (GH) family 6 CBH from *Phanerochaete chrysosporium* (*Pc*Cel6A) [22] and GH7 CBH from *Trichoderma reesei* (*Tr*Cel7A) [6] towards highly crystalline cellulose from green algae *Cladphora* spp. used in this study are taken from the cited references. Global fitting of the data was done using Igor Pro (ver. 8.04, Wavemetric, Inc.)

RESULTS AND DISCUSSION

Recent biophysical experiments using HS-AFM indicate that cellulases, especially processive enzymes, move along the substrate chains of crystalline cellulose [12–14], and biochemical results need to be reanalyzed to take account of the dynamics of the enzyme. However, as regards the parameters, Väljamäe and coworkers' stated "It must be pointed out that we do not attach any physical interpretation to these constants since they are empirical" [11], and this situation has not changed in the past quarter of a century. In the present manuscript, we take a bottom-up approach based on the molecular mechanism of the enzyme.

As shown in Fig. 1, cellulase molecules may exist in three states: in solution, and on cellulose in a non-productive or productive manner. Chemical equations for the process are written as

$$E_s \underset{k_{-1}}{\overset{k_1}{\rightleftarrows}} E_{np} \underset{k_{-2}}{\overset{k_2}{\rightleftarrows}} E_p + P$$

$$E_p \xrightarrow{k_3} E_s + \nu P$$

where E_s, E_{np}, E_p, and P are the concentrations of the enzyme molecule in solution, non-productively bound enzyme, productively bound enzyme, and the products, respectively. ν is the number of processive movements before the enzyme leaves from the cellulose surface. Note that we define the completion of productive binding when a cellulose chain is fully accommodated into the end of the tunnel in CD of the cellulase, simultaneously hydrolyzed and yielding a single cellobiose molecule [7]. Also, we assumed that the transition from non-productive binding to productive binding is reversible, given that this process is driven by the gradient of the potential energy, which could be perturbated by thermal fluctuations [23]. The following relationships hold, where E_0 is the total amount of enzyme in the reaction mixture:

$$E_s + E_{np} + E_p = E_0 \tag{1}$$

$$\dot{E}_{np} = k_1 E_s + k_{-2} E_p - k_{-1} E_{np} - k_2 E_{np} \tag{2}$$

$$\dot{E}_p = k_2 E_{np} - (k_{-2} + k_3) E_p \tag{3}$$

$$\dot{P} = k_2 E_{np} + \nu k_3 E_p \tag{4}$$

Note that in Eq. (2), the term for the transition from productive to non-productive binding was denoted as $k_{-2}E_p$ instead of $k_{-2}E_pP$ because this process only involves mechanical detachment and does not require the hydrolyzed cellobiose molecule. From Eqs. (1) and (2), and (1) and (3), we obtain the following relationships:

$$\begin{aligned}\dot{E}_{np} &= k_1(E_0 - E_p - E_{np}) + k_{-2}E_p - (k_{-1}+k_2)E_{np} \\ &= k_1 E_0 - (k_1 - k_{-2})E_p - (k_1 + k_{-1} + k_2)E_{np}\end{aligned} \tag{5}$$

$$\dot{E}_p = k_2 E_{np} - (k_{-2} + k_3)E_p \tag{6}$$

The following relationships are defined:

$$k_1 E_0 \equiv C_1$$

$$(k_1 - k_{-2}) \equiv C_2$$

$$k_1 + k_{-1} + k_2 \equiv C_3$$

$$k_2 \equiv C_4$$

$$k_{-2} + k_3 \equiv C_5$$

$$E_{np} \equiv x$$

$$E_p \equiv y$$

$$\dot{x} = C_1 - C_2 y - C_3 x \tag{7}$$

$$\dot{y} = C_4 x - C_5 y \tag{8}$$

From Eqs. (7) and (8),

$$\begin{aligned}\ddot{x} &= -C_2\dot{y} - C_3\dot{x} \\ &= -C_2(C_4 x - C_5 y) - C_3\dot{x} \\ &= -C_2 C_4 x + C_5(-\dot{x} - C_3 x + C_1) - C_3\dot{x}\end{aligned}$$

$$\ddot{x} + (C_3 + C_5)\dot{x} + (C_2 C_4 + C_3 C_5)x - C_1 C_5 = 0$$

$$\ddot{x} + (C_3 + C_5)\dot{x} + (C_2 C_4 + C_3 C_5)\left(x - \frac{C_1 C_5}{C_2 C_4 + C_3 C_5}\right) = 0$$

Simplifying, we have

$$x - \frac{C_1 C_5}{C_2 C_4 + C_3 C_5} \equiv X$$

$$\ddot{X} + (C_3 + C_5)\dot{X} + (C_2 C_4 + C_3 C_5)X = 0 \tag{9}$$

The eigenvalues of this second-order linear differential equation λ_1 and λ_2 are obtained as follows:

$$\lambda_1 + \lambda_2 = -(C_3 + C_5)$$

$$\lambda_1 \lambda_2 = (C_2 C_4 + C_3 C_5)$$

$$\lambda_1, \lambda_2 = \frac{-(C_3 + C_5) \pm \sqrt{(C_3 + C_5)^2 - 4(C_2 C_4 + C_3 C_5)}}{2}$$

$$= \frac{-(k_1 + k_{-1} + k_2 + k_{-2} + k_3) \pm \sqrt{(k_1 + k_{-1} + k_2 + k_{-2} + k_3)^2 - 4(k_1 k_2 + k_1 k_{-2} + k_1 k_3 + k_{-1} k_{-2} + k_{-1} k_3 + k_2 k_3)}}{2}$$

Given that E_s is generally much larger than E_{np} and E_p (since only cellulases near the surface of cellulose contribute to the reaction), in the situation where $k_1 < k_{-2}$ (i.e., $C_2 < 0$), both λ_1 and λ_2 become negative real numbers. This was confirmed by fitting to actual data as described later.

Thus, the solution of the differential Eq. (9) can be expressed as

$$X = \omega_1 e^{\lambda_1 t} + \omega_2 e^{\lambda_2 t},$$

and thus, we obtain

$$x=\omega_1 e^{\lambda_1 t}+\omega_2 e^{\lambda_2 t}+\frac{\left(k_1k_{-2}+k_1k_3\right)E_0}{k_1k_2+k_1k_{-2}+k_1k_3+k_{-1}k_{-2}+k_{-1}k_3+k_2k_3} \tag{10}$$

where ω_1 and ω_2 are constants satisfying the following relationships derived from $x(0)=0$ and $\dot{x}(0)=k_1E_0$, respectively:

$$\omega_1+\omega_2=-\frac{\left(k_1k_{-2}+k_1k_3\right)E_0}{k_1k_2+k_1k_{-2}+k_1k_3+k_{-1}k_{-2}+k_{-1}k_3+k_2k_3}$$

$$\lambda_1\omega_1+\lambda_2\omega_2=k_1E_0$$

Similar equations for y can also be derived from Eqs. (7) and (8):

$$\begin{aligned}\ddot{y}&=C_4\dot{x}-C_5\dot{y}\\&=C_4\left(C_1-C_2y-C_3x\right)-C_5\dot{y}\\&=C_1C_4-C_2C_4y-C_3\left(\dot{y}+C_5y\right)-C_5\dot{y}\end{aligned}$$

$$\ddot{y}+\left(C_3+C_5\right)\dot{y}+\left(C_2C_4+C_3C_5\right)y-C_1C_4=0$$

$$\ddot{y}+\left(C_3+C_5\right)\dot{y}+\left(C_2C_4+C_3C_5\right)\left(y-\frac{C_1C_4}{C_2C_4+C_3C_5}\right)=0$$

Simplifying, we have

$$y-\frac{C_1C_4}{C_2C_4+C_3C_5}\equiv Y$$

$$\ddot{Y}+\left(C_3+C_5\right)\dot{Y}+\left(C_2C_4+C_3C_5\right)Y=0 \tag{11}$$

Since Eq. (11) is similar to (9),

$$Y=\omega_3 e^{\lambda_1 t}+\omega_4 e^{\lambda_2 t}$$

$$y=\omega_3 e^{\lambda_1 t}+\omega_4 e^{\lambda_2 t}+\frac{k_1k_2E_0}{k_1k_2+k_1k_{-2}+k_1k_3+k_{-1}k_{-2}+k_{-1}k_3+k_2k_3} \tag{12}$$

where ω_3 and ω_4 are constants satisfying the following relationships derived from $\dot{y}(0)=0$ and $y(0)=0$, respectively:

$$\omega_3+\omega_4=-\frac{k_1k_2E_0}{k_1k_2+k_1k_{-2}+k_1k_3+k_{-1}k_{-2}+k_{-1}k_3+k_2k_3}$$

$$\lambda_1\omega_3+\lambda_2\omega_4=0$$

Finally, a differential equation for P is derived from Eqs. (4), (10) and (12);

$$\begin{aligned}\frac{dP}{dt}&=k_2x+\nu k_3y\\&=k_2\left(\omega_1e^{\lambda_1t}+\omega_2e^{\lambda_2t}+\xi_x\right)+\nu k_3\left(\omega_3e^{\lambda_1t}+\omega_4e^{\lambda_2t}+\xi_y\right)\\&=\left(k_2\omega_1+\nu k_3\omega_3\right)e^{\lambda_1t}+\left(k_2\omega_2+\nu k_3\omega_4\right)e^{\lambda_2t}+k_2\xi_x+\nu k_3\xi_y\end{aligned}$$

where

$$\xi_x=\frac{\left(k_1k_{-2}+k_1k_3\right)E_0}{k_1k_2+k_1k_{-2}+k_1k_3+k_{-1}k_{-2}+k_{-1}k_3+k_2k_3}$$

$$\xi_y=\frac{k_1k_2E_0}{k_1k_2+k_1k_{-2}+k_1k_3+k_{-1}k_{-2}+k_{-1}k_3+k_2k_3}$$

The equation is then integrated as

$$\int \frac{dP}{dt} \cdot dt = \frac{\mu_1}{\lambda_1} e^{\lambda_1 t} + \frac{\mu_2}{\lambda_2} e^{\lambda_2 t} + \mu_3 t + C_p$$

where

$$\mu_1 = k_2 \omega_1 + \nu k_3 \omega_3$$

$$\mu_2 = k_2 \omega_2 + \nu k_3 \omega_4$$

$$\mu_3 = k_2 \xi_x + \nu k_3 \xi_y$$

and C_p is a constant,
Using the initial condition, $P(t=0)=0$,

$$P = -\frac{\mu_1}{\lambda_1}\left(1 - e^{\lambda_1 t}\right) - \frac{\mu_2}{\lambda_2}\left(1 - e^{\lambda_2 t}\right) + \mu_3 t$$

$$= -\frac{k_2 \omega_1 + \nu k_3 \omega_3}{\lambda_1}\left(1 - e^{\lambda_1 t}\right) - \frac{k_2 \omega_2 + \nu k_3 \omega_4}{\lambda_2}\left(1 - e^{\lambda_2 t}\right) + \frac{k_1 k_2 k_{-2} + k_1 k_2 k_3 (1+\nu)}{k_1 k_2 + k_1 k_{-2} + k_1 k_3 + k_{-1} k_{-2} + k_{-1} k_3 + k_2 k_3} E_0 t \quad (13)$$

Therefore, Eq. (13) can be simplified into the following double-exponential form with a linear term as follows:

$$P(t) = \frac{a}{b}\left(1 - e^{bt}\right) + \frac{c}{d}\left(1 - e^{dt}\right) + f E_0 t \quad (14)$$

where $b < 0$, $d < 0$ and $f > 0$.

In the derivation of Eq. (14), there is no assumption that heterogeneity, i.e. amorphous or crystalline form of cellulose, or involvement of other enzymes such as EGs and CBHs plays a role. Instead, the double exponential equation simply arises from the reaction mechanism of single enzyme. However, we should point out that this does not exclude contributions of other factors such as those mentioned above. Nevertheless, a double exponential equation can be expected simply on the basis of the substrate/enzyme combination alone.

The progress curves of *Pc*Cel6A and *Tr*Cel7A were then re-analyzed using global fitting together with Eq. (14). Global fitting has recently been utilized to analyze enzyme kinetics because multiple parameters are optimized at once by non-linear regression. When the famous Michaelis-Menten study of sucrose hydrolysis by sucrase (invertase) was re-analyzed using this technique [24], it became apparent that substrate inhibition had not been considered in the initial kinetic study by Michaelis and Menten [25]. Moreover, we have applied global fitting to the complicated substrate loading system in processive cellulases [26]. Thus, global fitting is a powerful tool when multiple parameters must be considered. Since λ_1 and λ_2 (b and d in Eq. (14), respectively) are usually treated as rate constants and they do not include enzyme concentration (E_0), these parameters were

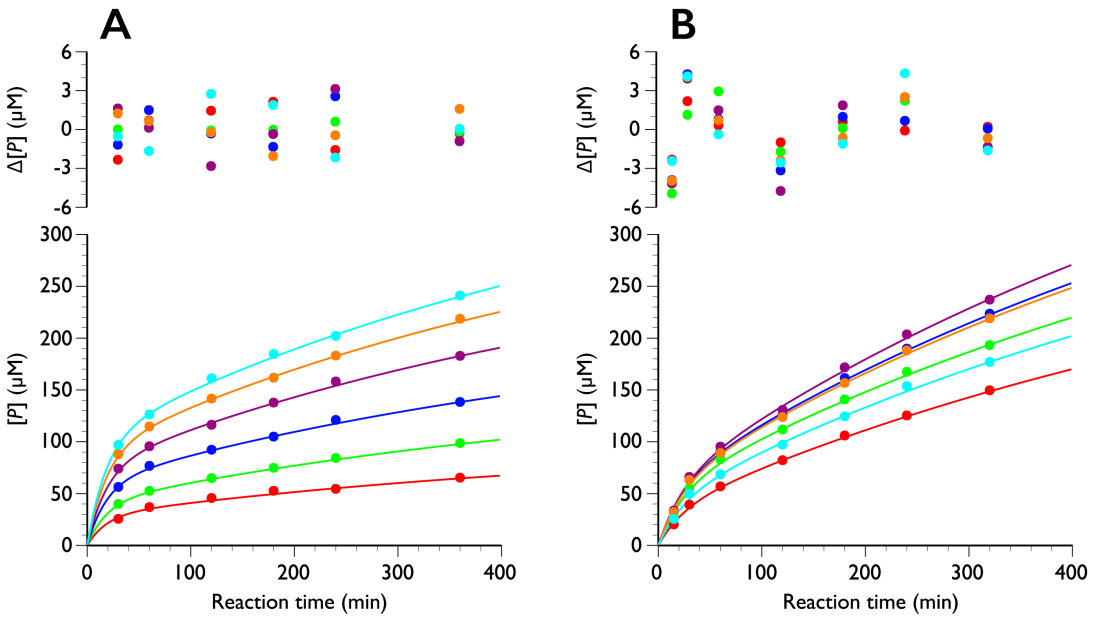

Fig. 2. Time course of product formation from crystalline cellulose Iα at 30 ˚C.
The progress curves of *Pc*Cel6A (A) and *Tr*Cel7A (B) were globally fitted to Eq. (14). The residue values between the experimental data and the curve fitting are shown above the plots. Red, green, blue, purple, orange and cyan are 0.25, 0.51, 1.0, 2.2, 5.4, and 8.9 μM for *Pc*Cel6A in (A), and 0.40, 0.84, 1.3, 2.2, 4.3, and 8.6 μM for *Tr*Cel7A in (B), respectively.

Table 1. Parameters of crystalline cellulose hydrolysis by *Pc*Cel6A estimated using global fitting.

E_0 (μM)	*a*	*b* (=λ_1)	*c*	*d* (=λ_2)	*a*/*b*	*c*/*d*
0.25	− 1.55 ± 0.12	− 0.0541	− 0.136 ± 0.015	− 0.00180	28.6 ± 2.0	75.5 ± 11.0
0.51	− 2.21 ± 0.14	± 0.0040	− 0.215 ± 0.021	± 0.00037	40.8 ± 2.3	120 ± 16
1.0	− 3.23 ± 0.18		− 0.297 ± 0.027		59.6 ± 2.8	165 ± 21
2.2	− 4.01 ± 0.20		− 0.410 ± 0.035		74.0 ± 3.4	228 ± 29
5.4	− 4.84 ± 0.24		− 0.478 ± 0.041		89.4 ± 3.8	265 ± 34
8.9	− 5.47 ± 0.27		− 0.525 ± 0.045		101 ± 4	291 ± 37

Table 2. Parameters of crystalline cellulose hydrolysis by *Tr*Cel7A estimated using global fitting without *f* in Eq. (14).

E_0 (μM)	*a*	*b* (=λ_1)	*c*	*d* (=λ_2)	*a*/*b*	*c*/*d*
0.40	− 1.33 ± 0.14	− 0.0412	− 0.455 ± 0.053	− 0.00146	32.2 ± 5.1	311 ± 81
0.84	− 2.13 ± 0.16	± 0.0062	− 0.556 ± 0.066	± 0.00053	51.6 ± 6.5	381 ± 97
1.3	− 2.33 ± 0.17		− 0.650 ± 0.076		56.5 ± 7.2	445 ± 114
2.2	− 2.35 ± 0.17		− 0.705 ± 0.081		57.1 ± 7.5	484 ± 124
4.3	− 2.28 ± 0.17		− 0.638 ± 0.075		55.5 ± 7.1	437 ± 112
8.6	− 1.68 ± 0.15		− 0.533 ± 0.062		40.7 ± 5.8	365 ± 95

Table 3. Parameters of crystalline cellulose hydrolysis by *Tr*Cel7A estimated using global fitting including *f* in Eq. (14).

E_0 (μM)	*a*	*b* (=λ_1)	*c*	*d* (=λ_2)	*f*	*a*/*b*	*c*/*d*
0.40	− 1.31 ± 0.15	− 0.0413	− 0.459 ± 0.057	− 0.00158	0.0108	31.7 ± 5.4	291 ± 87
0.84	− 2.11 ± 0.17	± 0.0063	− 0.555 ± 0.071	± 0.00064	± 0.0291	51.1 ± 6.8	353 ± 109
1.3	− 2.31 ± 0.18		− 0.644 ± 0.084			56.0 ± 7.5	409 ± 131
2.2	− 2.34 ± 0.18		− 0.689 ± 0.101			56.7 ± 7.7	437 ± 153
4.3	− 2.23 ± 0.17		− 0.590 ± 0.158			55.5 ± 7.2	375 ± 177
8.6	− 1.73 ± 0.21		− 0.422 ± 0.316			41.8 ± 6.8	268 ± 251

fixed at all enzyme concentrations tested, and other parameters were simulated from the data of *Pc*Cel6A [22] and *Tr*Cel7A [6] using Eq. (14) as shown in Fig. 2. The obtained parameters are listed in Tables 1–3.

As shown in Fig. 2, the progress curves of both enzymes are well fitted by the equation. In the case of *Pc*Cel6A, all progress curves at various enzyme concentrations (0.25 to 8.9 μM) were well fitted by Eq. (14) and the *f*-value converged to almost 0 ($<10^{-18}$). Therefore, the parameters were obtained using $f = 0$. From Eq. (13), this assumption implies that k_2, the rate of forming a productive binding, is significantly smaller than k_1 and k_3, which is reasonable considering the limited access to the reaction. On the other hand, progress curves of *Tr*Cel7A seem to include an *f*-value, though the errors of each parameter were large, especially for the second exponential term, *c* and *c*/*d*, possibly because the second exponential term and linear term are quite similar to each other. Therefore, we also analyzed the data using Eq. (14) without *f* (i.e., *f*=0) for *Tr*Cel7A. The rate constants of the two enzymes are rather similar, though that of *Pc*Cel6A is slightly faster, in agreement with reported data.

However, the enzyme concentration dependence of the amplitudes of the exponential terms, *a*/*b* and *c*/*d* values, are very different from each other. As shown in Fig. 3, the enzyme concentration dependence of both *a*/*b* and *c*/*d* was hyperbolic in the case of *Pc*Cel6A, while that of *Tr*Cel7A decreased with increasing enzyme concentration, which is similar to a typical substrate inhibition curve [27–29]. In a previous kinetic study of *Tr*Cel7A, we proposed possible crowding effects, and our hypothesis has been confirmed by biophysical HS-AFM and simulation studies [30]. Indeed, HS-AFM examination of processivity [15] indicated that the velocity of processive cellulase tends to decrease with increasing concentration of the enzyme, due to a "traffic jam" effect [13]. When we look at the construction of Eq. (14), most of the parameters except for λ_1 and λ_2 are dependent on E_0, and it is difficult to clarify the relationship between each parameter and E_0. However, it is clear that *a*/*b* and *c*/*d* are highly dependent on the amount of adsorbed enzyme, indicating that it is important to distinguish productive and non-productive adsorption.

In this paper, we modeled the formation of a productive binding event with the assumption that one product is generated. Even if we adopted the formulation including this term in the processive reaction, the conclusion that the time course of the product follows a double exponential form remains valid. This is because, in this case, the first term on the right side of Eq. (4) would be eliminated, making *P* dependent solely on E_p, which itself has a double exponential form.

So far, progress curves of cellulase have been fitted conventionally by a single or double exponential equation, or a single exponential equation with a linear function [6, 11]. Equation (14) includes all terms in those equations, and therefore curve-fitting with this equation is reasonable. Looking at the Eq. (13), however, several values, such as λ and ω, remain undetermined because the experimental data is not accurate enough. Nevertheless, it should be possible to estimate them individually, for

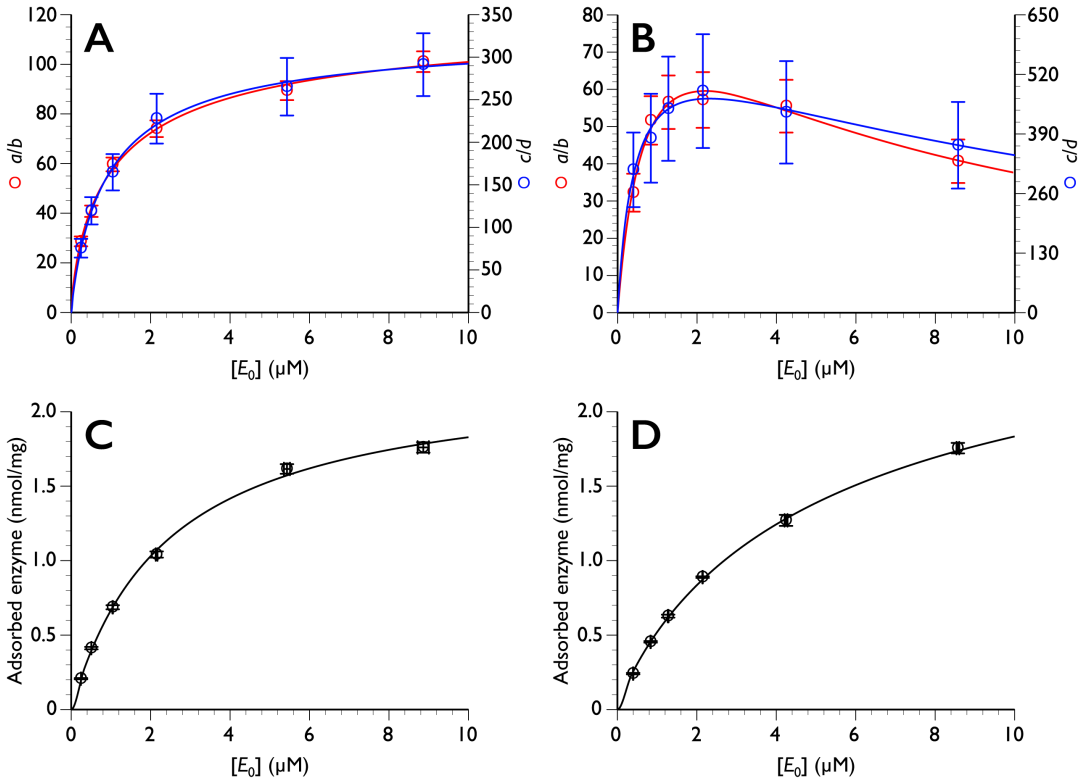

Fig. 3. The enzyme concentration dependence of both *a/b* and *c/d*.

Top: enzyme concentration (E_0) dependence of *a/b* and *c/d* for *Pc*Cel6A (A) and *Tr*Cel7A (B). Bottom: amount of adsorbed enzyme plotted *versus* E_0 for *Pc*Cel6A (C) and *Tr*Cel7A (D). The data in A, C, and D were fitted to typical hyperbolic curve ($y = (a \times x) / (b+x)$ where *a* and *b* are constants) while inhibition is considered ($y = (a \times x) / \{b+x+(x^2/c)\}$ where *a*, *b* and *c* are constants) in B. Note that the E_0 dependence of adsorption (C and D) does not correspond to a typical Langmuir plot of *ES versus* adsorbed enzyme.

example, by adsorption experiments for k_1/k_{-1} ratio, pre-steady-state kinetics for k_2/k_{-2}, processivity measurement by HS-AFM for *v*, and so on. Recently we succeeded in simulating approximately 100 million cellulase molecules using a customized traffic simulator and demonstrated that consideration of the dual domain structure of cellulase is indispensable to explain the gap between single-molecule behavior and bulk biochemical results [30]. In the simulation study, we defined the parameters for adsorption, non-productive and productive enzymes, and processivity, and the obtained progress curve fitted well to the actual biochemical plots, supporting the idea that theoretical and simulated approaches can give insight into real biophysical and biochemical observations.

In conclusion, we have constructed a mechanism-based equation that for the first time provides a theoretical basis for the double-exponential character of the progress curve of cellulase reaction. Thus, it is not necessary to consider the heterogeneity of the substrate or the involvement of multiple enzymes in order to explain the double-exponential nature of the progress curve, although we cannot rule out a contribution of such effects. We believe this work represents an important step towards understanding the actual saccharification of cellulosic biomasses. Furthermore, since the developed equation describes a model consisting of a simple enzymatic reaction at a solid/liquid interface, a similar approach may be appliable to many other enzymatic reactions involving insoluble substrates. The origin of the double exponential time course lies in a two-step reaction process involving long timescale equilibration. While such a form can arise in general two-step enzyme reactions, if the relaxation rates of each process are sufficiently fast, the behavior would effectively follow a single exponential.

CONFLICTS OF INTEREST

The authors declare no conflict of interests.

ACKNOWLEDGEMENTS

The authors thank Mr. Sho Sakuma in the University of Tokyo, who initiated the mathematical modelling of cellulase during his undergraduate research. This work was supported in part by Grants-in-Aid for Scientific Research (A) 23H00341 and (B) 19H03013 (to K.I.) from the Japan Society for the Promotion of Science (JSPS) and a Grant-in-Aid for Innovative Areas 18H05494 (to K.I.) from the Japanese Ministry of Education, Culture, Sports, and Technology (MEXT), and by the Environment Research and Technology Development Fund No. JPMEERF21S11900 and JPMEERF21S11902 (to K.I.) from the Environmental Restoration and Conservation Agency of Japan (ERCA).

REFERENCES

[1] Brandao AS, Goncalves A, Santos JMRCA. Circular bioeconomy strategies: From scientific research to commercially viable products. J Clean Prod. 2021; 295: 126407.

[2] Olivieri G, Wijffels RH, Marzocchella A, Russo ME. Bioreactor and bioprocess design issues in enzymatic hydrolysis of lignocellulosic biomass. Catalysts. 2021; 11: 680.

[3] Teeri TT, Koivula A, Linder M, Wohlfahrt G, Divne C, Jones TA. *Trichoderma reesei* cellobiohydrolases: why so efficient on crystalline cellulose? Biochem Soc Trans. 1998; 26: 173−8.

[4] Teeri TT. Crystalline cellulose degradation: New insight into the function of cellobiohydrolases. Trends Biotechnol. 1997; 15: 160−7.

[5] Sugimoto N, Igarashi K, Wada M, Samejima M. Adsorption characteristics of fungal family 1 cellulose-binding domain from *Trichoderma reesei* cellobiohydrolase I on crystalline cellulose: negative cooperative adsorption via a steric exclusion effect. Langmuir. 2012; 28: 14323−9.

[6] Igarashi K, Wada M, Hori R, Samejima M. Surface density of cellobiohydrolase on crystalline celluloses. A critical parameter to evaluate enzymatic kinetics at a solid-liquid interface. FEBS J. 2006; 273: 2869−78.

[7] Divne C, Ståhlberg J, Teeri TT, Jones TA. High-resolution crystal structures reveal how a cellulose chain is bound in the 50 Å long tunnel of cellobiohydrolase I from *Trichoderma reesei*. J Mol Biol. 1998; 275: 309−25.

[8] Divne C, Ståhlberg J, Reinikainen T, Ruohonen L, Pettersson G, Knowles JKC, et al. The 3-dimensional crystal-structure of the catalytic core of cellobiohydrolase I from *Trichoderma reesei*. Science. 1994; 265: 524−8.

[9] Wilson DB. Processive and nonprocessive cellulases for biofuel production-lessons from bacterial genomes and structural analysis. Appl Microbiol Biotechnol. 2012; 93: 497−502.

[10] Kipper K, Våljamåe P, Johansson G. Processive action of cellobiohydrolase Cel7A from *Trichoderma reesei* is revealed as 'burst' kinetics on fluorescent polymeric model substrates. Biochem J. 2005; 385: 527−35.

[11] Våljamåe P, Sild V, Pettersson G, Johansson G. The initial kinetics of hydrolysis by cellobiohydrolases I and II is consistent with a cellulose surface - erosion model. Eur J Biochem. 1998; 253: 469−75.

[12] Igarashi K, Koivula A, Wada M, Kimura S, Penttilå M, Samejima M. High speed atomic force microscopy visualizes processive movement of *Trichoderma reesei* cellobiohydrolase I on crystalline cellulose. J Biol Chem. 2009; 284: 36186−90.

[13] Igarashi K, Uchihashi T, Koivula A, Wada M, Kimura S, Okamoto T, et al. Traffic jams reduce hydrolytic efficiency of cellulase on cellulose surface. Science. 2011; 333: 1279−82.

[14] Igarashi K, Uchihashi T, Koivula A, Wada M, Kimura S, Penttilå M, et al. Visualization of cellobiohydrolase I from *Trichoderma reesei* moving on crystalline cellulose using high-speed atomic force microscopy. Methods Enzymol. 2012; 510: 169−82.

[15] Uchiyama T, Uchihashi T, Nakamura A, Watanabe H, Kaneko S, Samejima M, et al. Convergent evolution of processivity in bacterial and fungal cellulases. Proc Natl Acad Sci USA. 2020; 117: 19896−903.

[16] Sild V, Ståhlberg J, Pettersson G, Johansson G. Effect of potential binding site overlap to binding of cellulase to cellulose: A two-dimensional simulation. FEBS Lett. 1996; 378: 51−6.

[17] Eriksson KE, Pettersson B. Extracellular enzyme system utilized by fungus *Sporotrichum pulverulentum* (*Chrysosporium lignorum*) for breakdown of cellulose. 1. Separation, purification and physicochemical characterization of 5 Endo-1,4-β-glucanases. Eur J Biochem. 1975; 51: 193−206.

[18] Streamer M, Eriksson KE, Pettersson B. Extracellular enzyme-system utilized by fungus *Sporotrichum pulverulentum* (*Chrysosporium lignorum*) for breakdown of cellulose - Functional characterization of 5 endo-1,4-β-Glucanases and one exo-1,4-β-glucanase. Eur J Biochem. 1975; 59: 607−13.

[19] Almin KE, Eriksson KE, Pettersson B. Extracellular enzyme system utilized by fungus *Sporotrichum pulverulentum* (*Chrysosporium lignorum*) for breakdown of cellulose. 2. Activities of 5 endo-1,4-β-glucanases towards carboxymethylcellulose. Eur J Biochem. 1975; 51: 207−11.

[20] Coughlan MP. Mechanisms of cellulose degradation by fungi and bacteria. Anim Feed Sci Technol. 1991; 32: 77−100.

[21] Jalak J, Kurasin M, Teugjas H, Våljamåe P. Endo-exo synergism in cellulose hydrolysis revisited. J Biol Chem. 2012; 287: 28802−15.

[22] Igarashi K, Maruyama M, Nakamura A, Ishida T, Wada M, Samejima M. Degradation of crystalline celluloses by *Phanerochaete chrysosporium* cellobiohydrolase II (Cel6A) heterologously expressed in methylotrophic yeast *Pichia pastoris*. J Appl Glycosci. 2012; 59: 105−10.

[23] Mulakala C, Reilly PJ. Hypocrea jecorina (Trichoderma reesei) Cel7A as a molecular machine: A docking study. Proteins. 2005; 60: 598−605.

[24] Johnson KA, Goody RS. The original Michaelis constant: translation of the 1913 Michaelis-Menten paper. Biochemistry-Us. 2011; 50: 8264−9.

[25] Michaelis L, Menten ML. Die kinetik der invertinwirkung. Biochem Z. 1913; 49: 333−69.

[26] Nakamura A, Kanazawa T, Furuta T, Sakurai M, Saloheimo M, Samejima M, et al. Role of tryptophan 38 in loading substrate chain into the active-site tunnel of cellobiohydrolase I from *Trichoderma reesei*. J Appl Glycosci. 2021; 68: 19−29.

[27] Kawai R, Igarashi K, Kitaoka M, Ishii T, Samejima M. Kinetics of substrate transglycosylation by glycoside hydrolase family 3 glucan (1->3)-β-glucosidase from the white-rot fungus *Phanerochaete chrysosporium*. Carbohydr Res. 2004; 339: 2851−7.

[28] Igarashi K, Momohara I, Nishino T, Samejima M. Kinetics of inter-domain electron transfer in flavocytochrome cellobiose dehydrogenase from the white-rot fungus *Phanerochaete chrysosporium*. Biochem J. 2002; 365: 521−6.

[29] Igarashi K, Yoshida M, Matsumura H, Nakamura N, Ohno H, Samejima M, et al. Electron transfer chain reaction of the extracellular flavocytochrome cellobiose dehydrogenase from the basidiomycete *Phanerochaete chrysosporium*. FEBS J. 2005; 272: 2869−77.

[30] Ezaki T, Nishinari K, Samejima M, Igarashi K. Bridging the micro-macro gap between single-molecular behavior and bulk hydrolysis properties of cellulase. Phys Rev Lett. 2019; 122: 098102.